Hydrol. Earth Syst. Sci., 14, 159–169, 2010
www.hydrol-earth-syst-sci.net/14/159/2010/

Hydrology and Earth System Sciences

Climate and terrain factors explaining streamflow response and recession in Australian catchments

A. I. J. M. van Dijk

CSIRO Land and Water, Canberra, ACT, Australia

Received: 9 August 2009 – Published in Hydrol. Earth Syst. Sci. Discuss.: 14 September 2009
Revised: 5 January 2010 – Accepted: 8 January 2010 – Published: 27 January 2010

Abstract. Daily streamflow data were analysed to assess which climate and terrain factors best explain streamflow response in 183 Australian catchments. Assessed descriptors of catchment response included the parameters of fitted baseflow models, and baseflow index (BFI), average quick flow and average baseflow derived by baseflow separation. The variation in response between catchments was compared with indicators of catchment climate, morphology, geology, soils and land use. Spatial coherence in the residual unexplained variation was investigated using semi-variogram techniques. A linear reservoir model (one parameter; recession coefficient) produced baseflow estimates as good as those obtained using a non-linear reservoir (two parameters) and for practical purposes was therefore considered an appropriate balance between simplicity and explanatory performance. About a third (27–34%) of the spatial variation in recession coefficients and BFI was explained by catchment climate indicators, with another 53% of variation being spatially correlated over distances of 100–150 km, probably indicative of substrate characteristics not captured by the available soil and geology data. The shortest recession halftimes occurred in the driest catchments and were attributed to intermittent occurrence of fast-draining (possibly perched) groundwater. Most (70–84%) of the variation in average baseflow and quick flow was explained by rainfall and climate characteristics; another 20% of variation was spatially correlated over distances of 300–700 km, possibly reflecting a combination of terrain and climate factors. It is concluded that catchment streamflow response can be predicted quite well on the basis of catchment climate alone. The prediction of baseflow recession response should be improved further if relevant substrate properties were identified and measured.

Correspondence to: A. I. J. M. van Dijk
(albert.vandijk@csiro.au)

1 Introduction

The need to predict streamflow response where it is not observed is well established and an ongoing focus of hydrology research (e.g. Sivapalan et al., 2003). In the absence of streamflow observations, prediction requires an appropriate model and methods to estimate the model parameters. The focus of this paper is on the prediction of catchment baseflow behaviour. In unregulated rivers, baseflow (BF) is the dominant source of streamflow during periods of low rainfall. It is commonly assumed to originate from the groundwater store; the terms groundwater discharge and baseflow are often used interchangeably. The other component of total streamflow, storm flow or quick flow (QF) is interpreted to represent other, faster streamflow pathways, including infiltration excess and saturation overland flow, and unsaturated or saturated (perched) interflow. These are conceptual interpretations for which hydrographs per se cannot provide any proof, however.

Approaches to simulate baseflow recession in commonly used catchment models vary from single linear or non-linear stores to cascading or parallel groundwater stores (e.g. Bergström, 1992; Burnash et al., 1973; Chiew et al., 2002; Jakeman and Hornberger, 1993). The ability to reproduce observed baseflow recession patterns can be enhanced by increasing the number of stores or parameters to describe baseflow, but this also increases the likelihood of equivalence in the model structure or parameters (or "equifinality"; Beven, 1993). Estimating model parameters for ungauged catchments, commonly referred to as "regionalisation" (Blöschl and Sivapalan, 1995), can occur on the basis of spatial correlation in catchment behaviour or an established correlation with continuous or categorical measures of catchment climate, morphology, hydrogeology, soils or land use. Success in regionalisation is confounded when parameters are derived by calibrating under-determined model structures (Merz and Blöschl, 2004; Wagener and Wheater, 2006).

Published by Copernicus Publications on behalf of the European Geosciences Union.

The current study aims to assess what model complexity in baseflow description is justified when the only direct observations of catchment hydrological response are streamflow measurements; and to what extent streamflow behaviour can be predicted from catchment attributes and spatial correlation. This analysis was performed using a streamflow data for 183 unimpaired upland catchments in Australia. In particular, the following questions were posed:

- Is baseflow recession most parsimoniously described by a linear or by a non-linear reservoir equation?
- To what extent can variation in average baseflow, quick flow and the baseflow recession coefficient among catchments be related to catchment attributes?
- To what extent is the residual variability spatially correlated, and what are likely underlying factors?

It is beyond the aim of this paper to provide a review of the literature on recession modelling and methods for baseflow separation; good reviews are provided in Nathan and McMahon (1990), Tallaksen (1995), Wittenberg (1999) and Chapman (1999, 2003).

2 Theory

The method to separate daily streamflow data (Q, expressed as flow depth over the catchment area in mm d^{-1}) into baseflow (Q_{BF}) and quick flow (Q_{QF}) components requires a recession coefficient (k_{BF}) if a linear reservoir is assumed, and an additional, dimensionless exponent β if a non-linear reservoir is assumed. Both are described by:

$$Q_{BF} = -k_{BF} S^{\beta} \quad (1)$$

where S (mm) is reservoir storage. For a linear reservoir, β=1 and k_{BF} is expressed in d^{-1}; for a linear reservoir k_{BF} is expressed in mm$^{1-\beta}$ d^{-1}. It is assumed that quick flow only measurably affects streamflow during a period of T_{QF} days after the event peak flow, the length of which needs to be estimated in advance. Choosing T_{QF} too long reduces the amount of data and can lead to a bias in the results when baseflow behaviour is non-linear, whereas choosing the period too short introduces bias in the parameter estimates and subsequent streamflow separation due to the influence of QF on recession. Based on prior analysis it was considered that T_{QF}=10 days offers a useful compromise; the implications of this simplification will be revisited further on. For the analysis, all days showing an increase in Q from the previous day were considered to mark the start of a quick flow event. All these days as well as the T_{QF} days afterwards each of these events were excluded from the analysis. All days with zero flow or missing data were also excluded. From the remaining values, data pairs of Q and Q for the previous day (Q_*) were constructed.

For a non-linear reservoir, the relationship between initial storage (S_0 in mm) and S after t days is defined by:

$$S = S_0 \exp(-k_{BF} t) \quad (2)$$

Provided that both Q_* and Q represent baseflow only, Eqs. (1) and (2) can be combined and simplified by introducing $Q_0 = Q_*$ and t=1:

$$Q = Q_* \exp(-k_{BF}) \quad (3)$$

The derivation of an equivalent relationship for a non-linear reservoir is provided in Coutange (1948) and Wittenberg (1999) and produces:

$$Q = Q_* \left[1 + \frac{1-b}{ab} Q_*^{1-b} \right]^{\frac{1}{b-1}} \quad (4)$$

where the parameters expressed in terms of Eq. (1) are:

$$b = \frac{1}{\beta} \quad \text{and} \quad a = k_{BF}^{-b} \quad (5)$$

3 Methods

3.1 Data

Daily streamflow data (all expressed in ML day^{-1}) were collated for 260 catchments across Australia as part of previous studies (Guerschman et al., 2008; Peel et al., 2000). Streamflow data for these selected catchments were considered of satisfactory quality and any influence of river regulation, water extraction, urban development, or other processes upstream streamflow considered unimportant. Large lakes or wetlands do not occur in any of the catchments, but smaller impoundments can occur. The contributing catchments of all gauges were delineated through digital elevation model analysis and visual quality control (see Supplementary Material, http://www.hydrol-earth-syst-sci.net/14/159/2010/hess-14-159-2010-supplement.pdf). The streamflow data were converted to areal average streamflow (Q, mm d^{-1}).

Out of the overall data set, streamflow data were selected for 183 gauge records that for the period 1990–2006 had good quality observations for at least five consecutive years with less than 20% of data missing; no less than 50 runoff events (defined as an increase in streamflow from one day to the next); and no less than 50 $Q - Q_*$ data pairs remaining after removing zero-flow and quick flow affected data (T_{QF}=10 days). The maximum number of data pairs was 991, and the median 217.

The 183 stations are located along the east and southwest coast of Australia and mostly drain catchments with hard rock substrate and minor alluvial deposits (Fig. 1). Catchment areas vary between 51–1780 (median 313) km^2. The range of average annual precipitation is 408–2981 (median 923) mm y^{-1}, Priestley-Taylor potential evapotranspiration (E_0) varies from 651–2119 (median 1200) mm y^{-1} and average streamflow between 4–1936 (156) mm y^{-1}. Precipitation

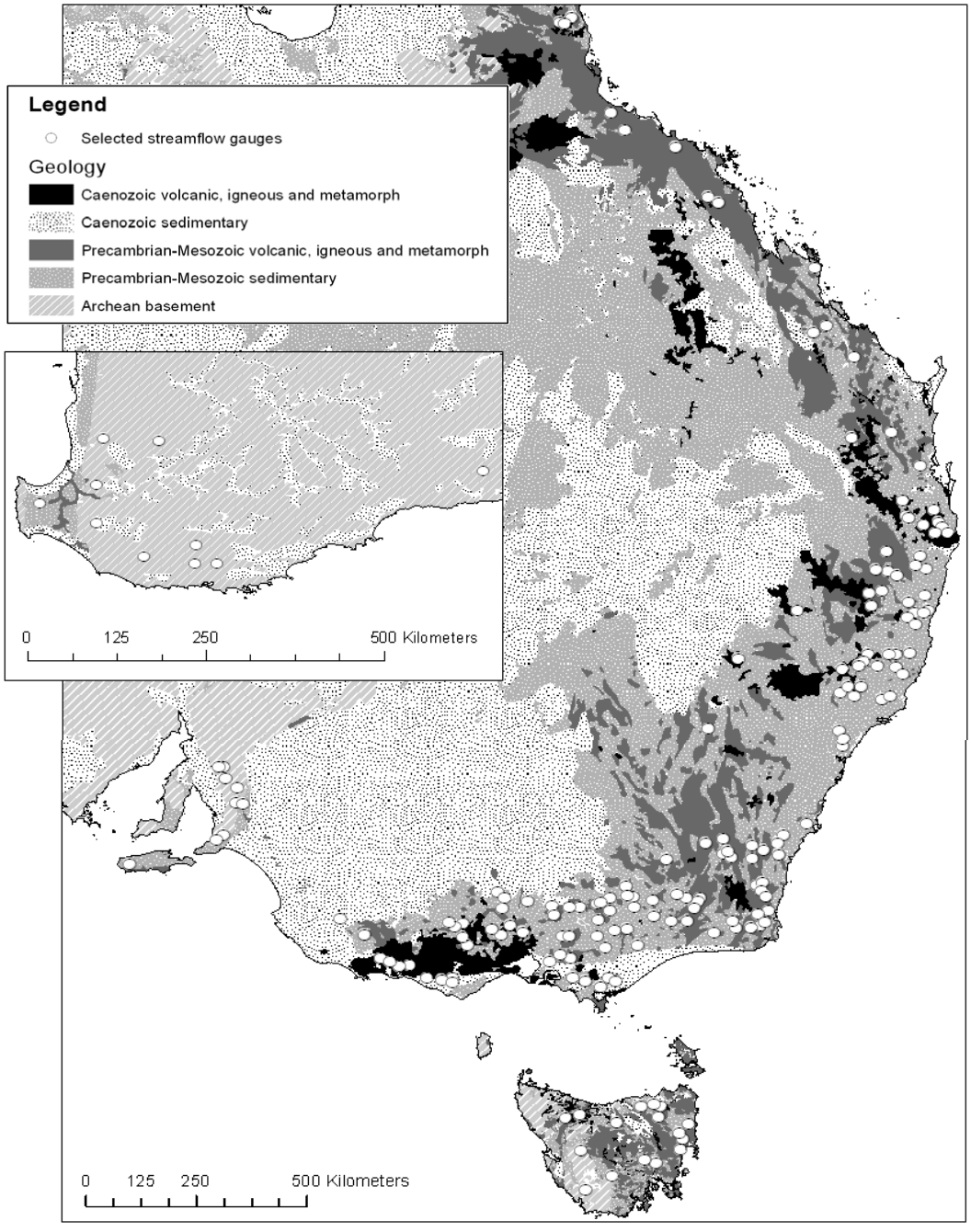

Fig. 1. The location of the 183 streamflow gauges selected in this study, and the underlying geology. Vector image provided separately.

other than rainfall was insignificant. The data set includes catchments under native forest, catchment fully cleared for grazing, and catchments with a varying combination of cropping, grazing, plantation forestry and native vegetation.

3.2 Parameter estimation

The parameter(s) of the linear and non-linear reservoir models were found by fitting Eqs. (3) and (4), respectively, to the available data pairs using a multi-start downhill simplex search method. The fitting criterion was the mean relative error (ε), expressed as:

$$\varepsilon = \frac{1}{n}\sum\left|\frac{Q_{\text{est}}}{Q} - 1\right| \tag{6}$$

where Q_{est} is Q predicted from Eqs. (3) or (4), respectively. This formulation gives equal weighting to all data pairs.

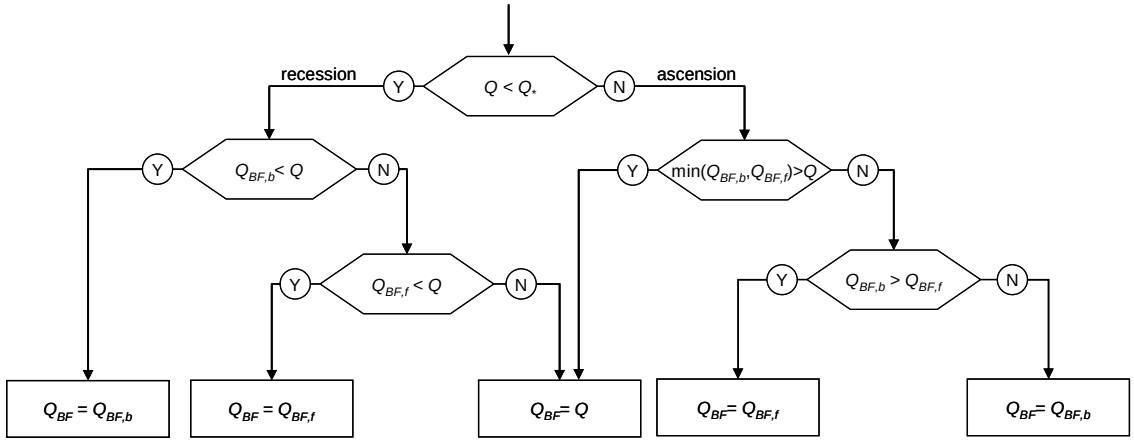

Fig. 2. Decision tree used in baseflow separation, where Q is streamflow, Q_* streamflow the previous day, and $Q_{\mathrm{BF,b}}$ the backward, $Q_{\mathrm{BF,f}}$ the forward and Q_{BF} the adopted baseflow estimate, respectively.

To investigate how the size of the data masking period T_{QF} influenced the results, the analysis was performed using a range of T_{QF} values for six stations selected to represent the geographical and climate range in the data set.

3.3 Model selection

To decide the optimal balance between the number of fitting parameters and explained variation in observations, a version of Akaike's Final Prediction Error Criterion (FPEC; Akaike, 1970) was calculated and interpreted. FPEC estimates the prediction error if the model was tested on a different data set and therefore the most accurate model should have the smallest FPEC. FPEC can be expressed as the product of an empirically estimated prediction error and a penalization factor that considers the degrees of freedom d (the number of free parameters) with the number of observations n (the number of data pairs). Provided that $n >> d$, FPEC is approximated by:

$$\mathrm{FPEC} = \frac{1+d/n}{1-d/n}\varepsilon \tag{7}$$

In principle, the model with the lowest FPEC should be adopted. For example, for n=50 (the lowest number of samples considered to produce a valid analysis), it follows that each additional parameter would need to explain another 4% of the residual error. Schoups et al. (2008) pointed out that this approach requires that n is very large or else may lead to underestimates of prediction error and favour overly complex models. This caveat was considered when interpreting FPEC values. The FPEC was not the only criterion used in deciding on appropriate model structure. Other factors considered were: (i) the number of stations for which the alternate model structure appeared to be better; (ii) any relationships between the number of data pairs and FPEC; (iii) the degree to which parameter values could be correlated to catchment attributes (increasing the likelihood of predictive performance in ungauged catchments); and (iv) the correlation between fitted parameters (as an indicator of potential parameter equivalence).

3.4 Baseflow separation

Using the chosen reservoir model and derived parameter values, the baseflow component of streamflow was estimated by combining forward and backward recursive filters. It was assumed that the very first and very last value in the streamflow time series represented baseflow only (associated errors were negligible).

Starting at the second last value of the stream flow time series ($i = N$–1) and moving backwards through the record, baseflow for time step i was estimated by considering forward and backward BF estimates. The forward estimate $Q_{\mathrm{BF,f}}$ is given by Eq. (3) for a linear reservoir and Eq. (4) for a non-linear reservoir; where $Q(i$–1) equalled zero, $Q_{\mathrm{BF,f}}(i)$ was also given a value of zero. The backward estimate $Q_{\mathrm{BF,b}}$ for a linear reservoir is given by inversion of Eq. (3) as:

$$Q_{\mathrm{BF,b}}(i) = \exp(k_{\mathrm{BF}})\, Q_{\mathrm{BF}}(i+1) \tag{8}$$

and for a non-linear reservoir as (cf. Eq. (4); Wittenberg, 1999):

$$Q_{\mathrm{BF,b}}(i) = \left\{ [Q_{\mathrm{BF}}(i+1)]^{b-1} + \frac{b-1}{ab} \right\}^{\frac{1}{b-1}} \tag{9}$$

To decide whether to assign the backward or forward baseflow estimate, the decision tree shown in Fig. 2 was used. An example result for a linear reservoir is shown in Fig. 3. After baseflow separation, period average BF and QF were calculated, as well as baseflow index (BFI), calculated as the ratio of total baseflow over total streamflow.

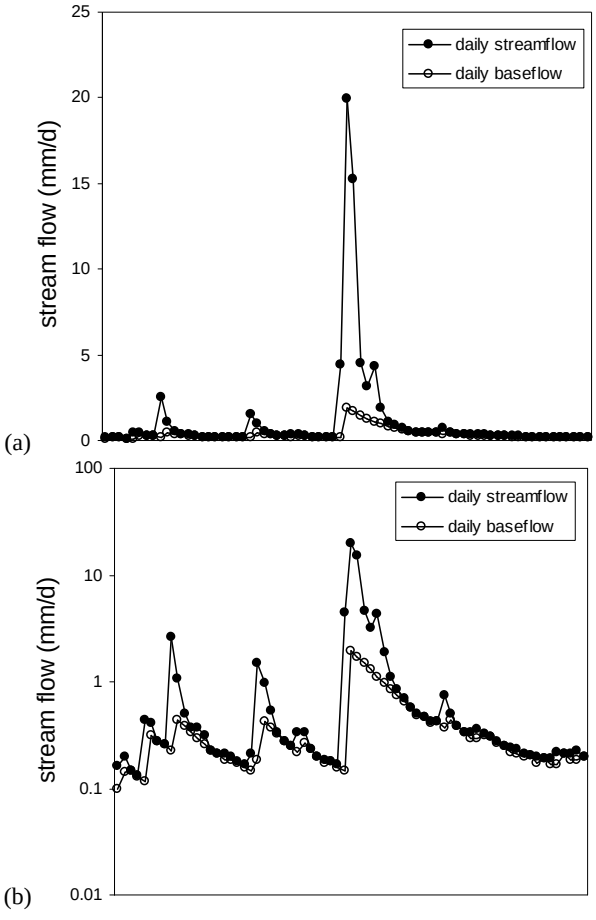

Fig. 3. Example of separation of daily streamflow into baseflow and storm flow using a linear baseflow reservoir , plotted on **(a)** a linear vertical scale and **(b)** a logarithmic vertical scale (data chosen arbitrarily to illustrate concepts; represent 60 days in winter 1990; gauge 410705, Molonglo River @ Burbong Bridge).

3.5 Spatial predictors of streamflow response

The streamflow response descriptors analysed were the reservoir model parameters (k_{BF} and β), BFI, and average QF and BF. Only categorical information was available on geology (Fig. 1). The mean and standard deviation of the values for catchments within each geological category were compared for statistically significant differences.

For other catchment characteristics continuous data was available, including measures of catchment morphology (catchment size, mean slope, flatness); soil characteristics (saturated hydraulic conductivity, dominant texture class value, plant available water content, clay content, solum thickness); climate indices (mean precipitation P, mean potential evapotranspiration E_0, humidity index $H = P/E_0$, remotely sensed actual evapotranspiration, average monthly excess precipitation); and land cover characteristics (fraction woody vegetation, fractions non-agricultural land, grazing land, horticulture, and broad acre cropping, remotely sensed vegetation greenness). Data sources are listed in the supplementary material (http://www.hydrol-earth-syst-sci.net/14/159/2010/hess-14-159-2010-supplement.pdf). The analysis involved step-wise regression: potential predictors of variation in the response descriptor were chosen based on parametric and non-parametric (ranked) correlation coefficients (r and r^*, respectively). A threshold of ± 0.40 (equivalent to r^2=0.20) was considered a potentially meaningful correlation. Linear, logarithmic, exponential and power regression equations were calculated for all potential predictors, and the most powerful one selected. The residual variance was calculated and expressed both as absolute and relative residuals, after which the same procedure was repeated.

When no further variation could be explained by the catchment attributes, the spatial correlation in the remaining residual variance was investigated using semi-variograms. A minimum of 100 unique member data points was used for each variogram estimator point and a spherical, exponential or linear semi-variogram model was visually selected and fitted. The ratio of sill over the sum of sill and nugget was interpreted as the fraction of total variance that appeared spatially correlated, and the range of the variogram model was interpreted as the characteristic length scale of correlation. The same semi-variogram analysis was also was performed for the various catchment attributes (see supplementary material, http://www.hydrol-earth-syst-sci.net/14/159/2010/hess-14-159-2010-supplement.pdf). The range of the variogram was interpreted as the characteristic length scale of correlation, suggesting that available data on soils, topography, major land uses and vegetation cover had typical correlation lengths of 100 to 300 km, whereas climate and potential evaporation showed length scales of 300 to 700 km. The semi-variogram suggested no spatial correlation in catchment size or the area with different crops.

4 Results

4.1 Parameter estimation

The influence of the choice of masking period T_{QF} on calculated k_{BF} values and the number of available data pairs is illustrated for six stations in Fig. 4a–f. Calculated k_{BF} falls rapidly as T_{QF} is increased to 7–14 days, and a minimum value is calculated if T_{QF} is set to 7–28 days (Fig. 4a and b, respectively). The number of available data pairs reduces exponentially as greater T_{QF} values are chosen, and no data remains for T_{QF} of 20–40 days (Fig. 4b and d, respectively). For T_{QF} values greater than 10 days calculated k_{BF} values show variable and sometimes complex trends (e.g. Fig. 4a and f), but the remaining number of data pairs becomes increasingly small and likely to be associated with a single or small number of long baseflow recessions. Overall, setting T_{QF} at 10 days was considered a reasonable compromise that maximised data availability whilst avoiding undue influence from storm flow recession.

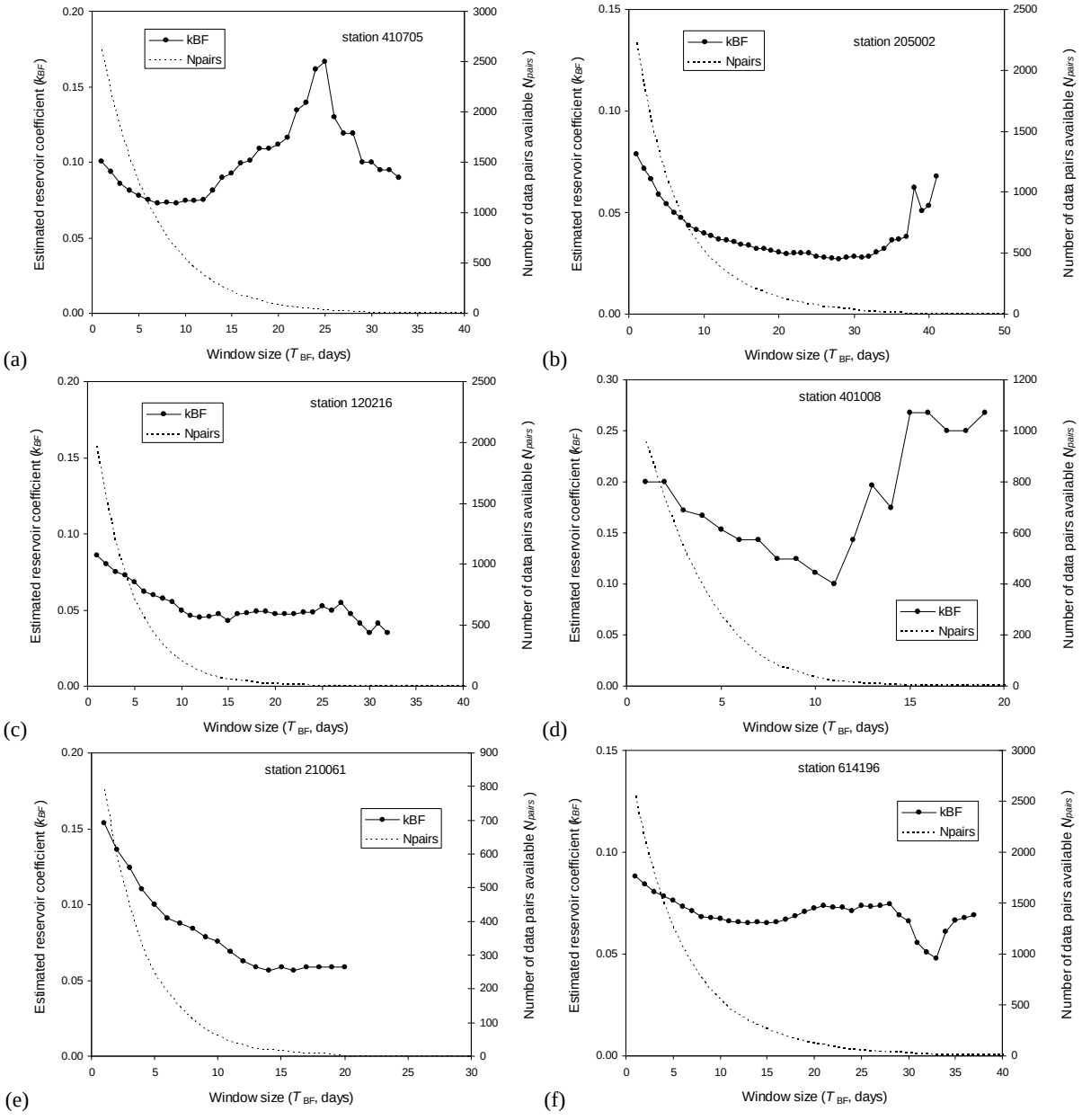

Fig. 4. Example k_{BF} values derived (closed lines) and number of Q/Q_* pairs (dotted line) as the length of the storm flow masking window T_{BF} is increased from zero to 50 days. The six stations shown were selected to cover different geographical areas and climate regimes.

Fitting the linear reservoir model produced an average k_{BF} of 0.0596 (st. dev. $\pm$0.0288), implying a half-time of about 12 days. Values appeared approximately log-normally distributed (Fig. 5) and 80% of values were in the range 0.030–0.095 (i.e. half-times of 7–23 days). Fitting a non-linear reservoir produced a median β value of 0.95. The distribution was strongly skewed; 50% of values were between 0.82–1.26 and 80% of values between 0.70–1.83 (Fig. 5). Seemingly unrealistic values of $\beta \geq 4$ were derived for eight stations and values of $\beta \leq 0.50$ found for four stations. Corresponding values of k_{BF} appeared normally distributed, and produced an average value of k_{BF}=0.0567 (st. dev. $\pm$0.0407); 80% of all values was between 0.0012–0.1147. There was correlation between k_{BF} and β values (non-parametric r^*=−0.75). There was also correlation between the respective k_{BF} values for the linear and non-linear reservoir model (r^*=0.76).

Table 1. Summary of the analysis of variance in values derived from baseflow separation for the 183 catchments. Listed are the fraction of variance explained by catchment attributes, the residual variance showing spatial correlation and the remaining unexplained variance. Also listed are the range (km) of the fitted semi-variograms (provided in supplementary material, http://www.hydrol-earth-syst-sci.net/14/159/2010/hess-14-159-2010-supplement.pdf).

		Fraction of variance			
Variable	Symbol	Attributed	Spatially correlated	Unexplained	Range (km)
Recession coefficient	k_{BF}	27%	53%	20%	200
Baseflow index	BFI	34%	53%	13%	300
Base flow	Q_{BF}	84%	0%	16%	*n/a*
Quick flow	Q_{QF}	70%	20%	10%	400

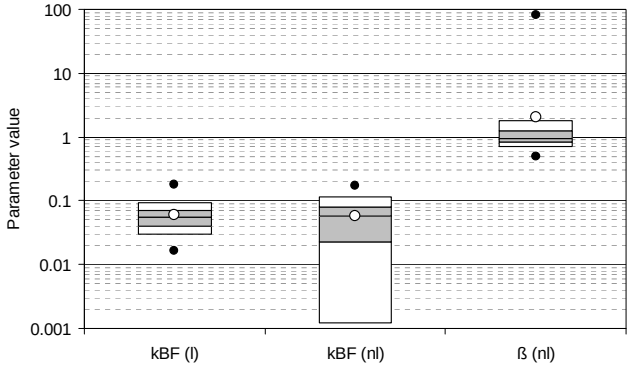

Fig. 5. Distribution of derived parameter values (N=183), from left to right, k_{BF} for a linear reservoir (l) and for a non-linear reservoir (nl) and the fitted value of β for the non-linear reservoir. Shown are the mean (open dot), minimum and maximum (closed dots), 10–90% range (white bars), and the 25, 50 and 75% percentiles (shaded bars). Note logarithmic vertical axis.

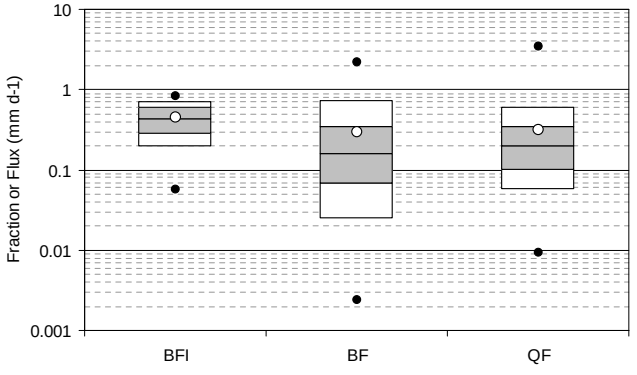

Fig. 6. Distribution of values of (from left to right) baseflow index (BFI), average baseflow (BF) and average quick flow (QF, both in mm d^{-1}) derived by baseflow separation using a linear reservoir. Shown are the mean (open dot), minimum and maximum (closed dots), 10–90% range (white bars), and the 25, 50 and 75% percentiles (shaded bars). Note the logarithmic vertical axis.

4.2 Model selection

The linear reservoir produced a median FPEC of 0.0306 and the non-linear reservoir a median FPEC of 0.0294, suggesting that the non-linear reservoir model reduced estimation error by 4%. The linear reservoir produced lower FPEC scores for 131 out of 183 stations, however. The parameter β could not be correlated to any catchment attribute (the greatest r^* was -0.31 with E_0). Values were within 20% of unity for 88 out of 183 stations, and outside the range of 0.5–4 for 12 stations. For the purposes of this study, these findings were considered insufficient basis to prefer the more complex and less robust non-linear reservoir model over the simpler linear reservoir model. Results presented from here onwards were obtained using the linear reservoir model unless stated otherwise.

4.3 Streamflow components

The distribution of catchment baseflow index (BFI) values appeared normal by approximation, with an average BFI of 0.45 (st. dev. $\pm$0.19; Fig. 6). The average BFI calculated using the non-linear reservoir model was 0.42$\pm$0.21. The median relative difference between the two BFI estimates was 5%, and the absolute error less than 0.10 for 162 out of 183 stations (including the 12 that had unrealistic values of β) The distribution of baseflow and quick flow averages was positively skewed. Median baseflow was 0.16 mm d^{-1} and median quick flow 0.20 mm d^{-1} (Fig. 6).

4.4 Spatial predictors of streamflow response

The results of step-wise regression and semi-variogram analysis are summarised in Table 1. Statistical analysis suggested no significant differences between different geology classes for any of the streamflow response descriptors.

The best predictor of k_{BF} was catchment humidity (r^*=0.60); comparatively slower recessions (smaller k_{BF}) occurred in more humid catchments. There was no correlation with catchment size (r^* =0.06). A power-relationship with catchment humidity explained 27% of the variance (Fig. 7). The residual variance was greater for drier catchments but was not explained by catchment attributes. Another 53% of total variance (i.e. 72% of

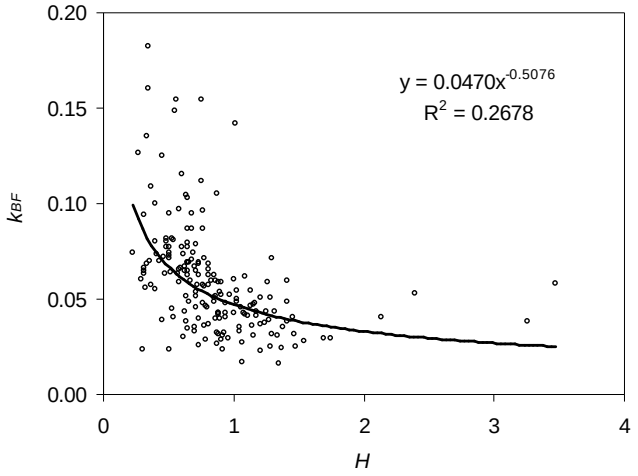

Fig. 7. Regression between humidity index H and the linear recession coefficient k_{BF}.

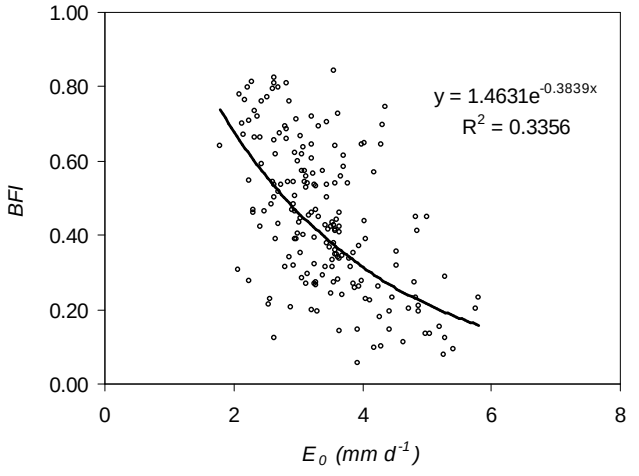

Fig. 8. Regression between E_0 and the period average baseflow index BFI.

residual variance) was spatially correlated with a characteristic length scale of 200 km (see supplementary material for all semi-variograms, http://www.hydrol-earth-syst-sci.net/14/159/2010/hess-14-159-2010-supplement.pdf). The remaining 20% of variance remained unexplained.

The best predictor of BFI was potential evapotranspiration (E_0, $r^* = -0.55$), but humidity, precipitation-weighted monthly humidity index, and the coefficient of variance in monthly precipitation were similarly good predictors (r^*=0.51–0.54). An exponential relationship explained 34% of the variance, having a standard error of estimate of $\pm$0.16 (Fig. 8). The residual variance was not explained by the remaining attributes, but another 53% of variance (81% of residual variance) was spatially correlated with a characteristic length scale of 300 km. The remaining 13% of variance was left unexplained.

The best predictor of BF was average monthly excess precipitation (AMEP, r^*=0.91), followed by H (r^*=0.88) and average rainfall and precipitation-weighted monthly humidity index (both r^*=0.84). A power relationship explained 84% of the variance (Fig. 9). The residual variance appeared spatially uncorrelated.

The best predictor of QF was rainfall (r^*=0.70); a power relationship explained 70% of the variance (Fig. 10). The coefficient of variation in monthly precipitation (r^*=0.36) and rainfall-weighted event precipitation (r^*=0.35) were the strongest predictors of the residual variance, but including them did not improve estimates. Another 20% of total variance (66% of residual variance) was spatially correlated over length scales of 400 km. The remaining 10% of variance was left unexplained.

5 Discussion

5.1 Selection of storm flow window

Streamflow during the first 7 to 10 days after storm flow events appeared to include rapid drainage of stores associated with the storm event, with longer recession times occurring in wetter catchments. The gradual increase in calculated k_{BF} when the masking period T_{QF} was increased beyond 10 to 30 days may reflect non-linear storage behaviour in the remaining low flow regime, but may also be caused by the greater influence of stream and riparian evapotranspiration losses in this regime (see below). The number of available data pairs often became very small as window size was increased further, introducing uncertainty and bias into the analysis. A window of 10 days was considered a reasonable compromise. The examples shown indicate that there is usually still some uncertainty.

5.2 Linear and non-linear storage behaviour

Fitting a linear reservoir produced results that were similar when compared to those obtained with a non-linear reservoir. The derived β values were generally close to unity and the use of an additional parameter did little to explain more variance in the observations. In addition, resulting parameter estimates sometimes appeared unrealistic. Baseflow separation using a linear reservoir also produced estimates of baseflow that were very similar to those obtained with a non-linear reservoir. Overall, for the purposes of this study there was considered to be little benefit from applying the more complex non-linear reservoir model.

Even so, there was some evidence in the data for non-linear storage behaviour (Fig. 4). Previous studies have argued for the use of non-linear reservoirs based on evidence of greater k_{BF} values for low flow conditions. Following

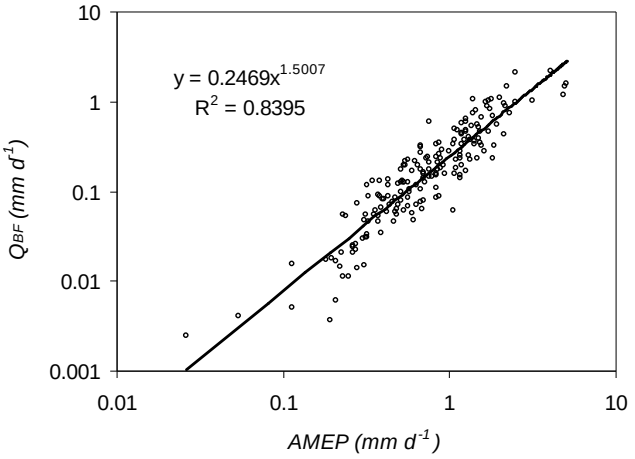

Fig. 9. Regression between average monthly excess precipitation (AMEP) and the period average baseflow (BF in mm d^{-1}) (note double logarithmic scale).

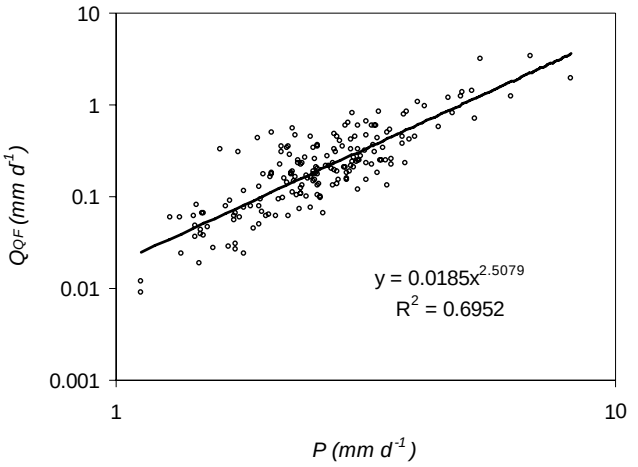

Fig. 10. Regression between average precipitation (P) and the period average quick flow (QF in mm d^{-1}).

Weisman (1977) and Tallaksen (1995), Wittenberg and Sivapalan (1999) argued that evapotranspiration from the river and riparian zone will lead to an accelerating recession at low baseflow levels, leading to fitted values of $\beta < 1$. After controlling for this effect, they found values of β between 2 and 3 (b=0.3–0.5). Similar values are commonly found in other countries and could be physically explained by convergence of flow paths (Chapman, 2003; Wittenberg, 1999). Where riparian evapotranspiration affects baseflow noticeably, seasonal differences in recession rates may also be expected (cf. Wittenberg and Sivapalan, 1999)

5.3 Predictability of recession coefficient

Of the variance in k_{BF} between stations, 27% could be attributed to humidity, 53% was correlated over length scales indicative of terrain factors (ca. 100 km), and 20% remained unexplained (Table 1). A priori, correlation might be expected with catchment size or geology, but no such relationship appeared to exist. On theoretical arguments, Zecharias and Brutsaert (1988) argued that the recession coefficient k_{BF} should be proportional to:

$$k_{\mathrm{BF}} \propto \frac{K D \alpha}{Y L} \tag{10}$$

where K is hydraulic conductivity, D aquifer thickness, α is slope, Y is storativity, and L a characteristic flow path length. Zecharias and Brutsaert (1988) and Brandes et al. (2005) found that geomorphological indices such as drainage density (a proxy for L), slope and hydrologic soil class (perhaps a proxy for K and S) together explained about 70–80% of the variation in k_{BF} for catchments in the Appalachians (USA). In the current study, catchment-average saturated conductivity and slope estimates were available and showed weak correlations with k_{BF} ($r*$ of -0.30 and -0.41, respectively), but these relationships were opposite to those that would be expected. This was because of their correlation with catchment humidity; after correcting for this soil conductivity and slope did not explain any residual variance. Most of the variation in k_{BF} explained by the humidity index was for dry catchments ($H < 1$) with times of less than 10 days ($k_{\mathrm{BF}} > 0.07$; Fig. 7). These catchments generally had low average baseflow (<30 mm y^{-1}) and intermittent streamflow. It is concluded that the value of humidity in predicting k_{BF} is mainly due to the intermittent occurrence of (perched) groundwater tables with short half times in drier catchments.

The influence of perched groundwater tables, as well as perhaps the large geographical area and wide climate and geology range covered by the 183 catchments, may have prevented detection of the influence of hydrogeology and geomorphology on k_{BF}. The finding that there was considerable correlation of k_{BF} over a relatively short length scales of 200 km does suggest that there are spatial terrain factors underlying the variation in k_{BF}, but these were not captured in the catchment data available.

5.4 Predictability of base flow index

Catchment climate factors could explain 34% of the variation in BFI; another 53% of the variation was spatially correlated, while 13% of variation remained unexplained (Table 1). For the conterminous USA, Santhi et al. (2008) reported BFI values of similar range and average as those reported here. They found elevation and percentage sand were the strongest predictors of BFI, being negatively and positively related to BFI, respectively. The national maps of BFI (re)produced by Santhi et al. (2008) do however suggest that perhaps precipitation (or possibly the fraction of this falling as snow) may have been an important underlying factor. For the Elbe Basin (Germany), Haberlandt et al. (2001) were able to explain ca. 80% of the variance in BFI values using a

combination of catchment-average slope, topographic wetness index, rainfall, and soil conductivity. In the current analysis, direct evidence for a relationship between BFI and catchment-attributes relating to geomorphology or soils was not found, but there was considerable correlation over up to 150 km that may reflect undescribed terrain factors.

5.5 Predictability of average baseflow and storm flow

The overriding importance of rainfall and catchment humidity in determining total streamflow is well documented (e.g. Oudin et al., 2008; van Dijk et al., 2007; Zhang et al., 2004). The current analysis shows that this extends to both BF and QF components. The standard error of estimate (SEE) using the first order regression models shown in Figs. 8 and 10 in different combinations to estimate baseflow and quick flow were both of similar magnitude but errors appeared uncorrelated. Estimates of BF were slightly more robust than QF estimates (SEE 70–87 vs. 89–94 mm y^{-1}; mean relative error 37–45 vs. 52–63%; r^*=0.89–0.92 vs. 0.67–0.76).

The empirical relationships derived provide some insight into the main drivers of spatial patterns in average baseflow, storm flow, and base flow index. The stronger explanatory value of monthly rainfall excess in predicting BF suggests that seasonality in rainfall relative to E_0 may be important in determining baseflow generation. Average quick flow showed a strongly non-linear relation with rainfall (exponent of 2.51; Fig. 10). This flow component could include several runoff generation mechanisms, including infiltration and saturation excess surface runoff and subsurface storm flow. Correspondingly, a multitude of factors may affect quick flow generation, including rainfall intensity distribution, factors affecting soil infiltration capacity (soil type but also land use and management), factors affecting saturated catchment area (antecedent groundwater level, geomorphology) and soil saturation (soil conductivity and structure, antecedent soil water content). It may be assumed that average rainfall intensity is positively related to total rainfall, whereas groundwater level and soil moisture content are likely to be higher in wetter catchments, providing several alternative hypotheses to explain the non-linear relationship between rainfall and QF found here.

6 Conclusions

Daily streamflow data for 183 catchments across Australia were used to estimate baseflow and quick flow contributions. Both linear and non-linear reservoirs were evaluated. Variations in reservoir parameters, baseflow index (BFI) and average baseflow and quick flow between the stations were analysed and where possible related to the climate, terrain and land cover attributes of the catchments using step-wise regression and semi-variogram techniques. The following conclusions are drawn:

1. A one-parameter linear reservoir produced estimates of baseflow that were as good as those obtained using a two-parameter non-linear reservoir. Because it had fewer parameters and parameter values that were less variable the linear reservoir model was considered preferable for the purposes of this study.

2. The transition from storm flow dominated streamflow to baseflow dominated streamflow generally appeared to occur between 7 and 10 days after storm events. The 183 catchments showed baseflow half-times of around 12 days, with 80% of stations having half-times of 7 to 23 days. Catchment humidity explained 27% of the variation in derived recession coefficients. The shortest half-times occurred in the driest catchments and were attributed to the occurrence of fast-draining (perched) groundwater.

3. Median BFI was 0.45, with considerable variation between stations. About half (53%) of the unexplained variance in recession coefficients and BFI values showed spatial correlation over scales of 100–150 km, probably associated with terrain factors that were not captured in the available data. The remaining 16–20% of variance in k_{BF} and BFI remained unexplained.

4. Most (84%) of the variation in average baseflow between stations could be explained by monthly precipitation in excess of E_0. Most (70%) of the variation in average quick flow between stations could be explained by average rainfall. Of the remaining variation, 20% was spatially correlated over spatial scales of ∼200 km, and this may reflect a combination of terrain and climate factors. The remaining 10–16% was left unexplained.

It is concluded that catchment streamflow response can be predicted quite well on the basis of catchment climate alone. The prediction of baseflow recession response should be improved further if relevant substrate properties were identified and measured.

Acknowledgements. This work is part of the water information research and development alliance between CSIRO's Water for a Healthy Country Flagship and the Bureau of Meteorology. The streamflow and catchment attribute data set used in this study was brought together by Juan Pablo Guerschman, Jorge Peña Arancibia, Yi Liu and Steve Marvanek of CSIRO Land and Water; their effort is gratefully acknowledged. This manuscript has benefited considerably from comments by Zahra Paydar and Cuan Petheram (CSIRO Land and Water), three anonymous referees and the subject editor.

Edited by: A. Montanari

References

Akaike, H.: Statistical predictor identification Ann. Inst. Stat. Math., 22, 203–217 doi:10.1007/BF02506337, 1970.

Bergström, S.: Bergstrom, S.: The HBV model – its structure and applications, Report RH No. 4, Swedish Meteorological and Hydrological Institute, Hydrology, Norrkping, Sweden, 35 pp. 1992.

Beven, K.: Prophecy, reality and uncertainty in distributed hydrological modelling, Adv. Water Resour., 16, 41–41, 1993.

Blöschl, G. and Sivapalan, M.: Scale issues in hydrological modelling: A review, Hydrol. Process., 9, 251–290, 1995.

Brandes, D., Hoffmann, J. G., and Mangarillo, J. T.: Base flow recession rates, low flows, and hydrologic features of small watersheds in Pennsylvania, USA, J. Am. Water Resour. As., 41, 1177–1186, 2005.

Burnash, R. J. C., Ferral, R. L., and McGuire, R.: A Generalized Streamflow Simulation System-Conceptual Modeling for Digital Computers, U.S. Department of Commerce, National Weather Service and State of California, Department of Water Resources, 1973.

Chapman, T.: A comparison of algorithms for stream flow recession and baseflow separation, Hydrol. Process., 13, 701–714, 1999.

Chapman, T. G.: Modelling stream recession flows, Environ. Modell. Softw., 18, 683–692, 2003.

Chiew, F. H. S., Peel, M. C., and Western, A. W.: Application and testing of the simple rainfall-runoff model SIMHYD, in: Mathematical Models of Small Watershed Hydrology and Applications, edited by: Singh, V. P. and Frevert, D. K., Water resources Publication Littleton, Colorado, USA, 335–367, 2002.

Coutagne, A.: Etude générale des variations de débits en fonction des facteurs qui les conditionnent, 2éme partie: les variations de débit en période non infuencée par les précipitations, La Houille Blanche, 416–436, 1948.

Guerschman, J.-P., Van Dijk, A. I. J. M., McVicar, T. R., Van Niel, T. G., Li, L., Liu, Y., and Peña-Arancibia, J.: Water balance estimates from satellite observations over the Murray-Darling Basin, CSIRO, Canberra, Australia, 93 pp., 2008.

Haberlandt, U., Klöcking, B., Krysanova, V., and Becker, A.: Regionalisation of the base flow index from dynamically simulated flow components – a case study in the Elbe River Basin, J. Hydrol., 248, 35–53, 2001.

Jakeman, A. J. and Hornberger, G. M.: How much complexity is warranted in a rainfall-runoff model?, Water Resour. Res. 29, 2637–2649, 1993.

Merz, R. and Blöschl, G.: Regionalisation of catchment model parameters, J. Hydrol., 287, 95–123, 2004.

Nathan, R. J. and McMahon, T. A.: Evaluation of automated techniques for base flow and recession analyses, Water Resour. Res., 26, 1465–1473, 1990.

Oudin, L., Andréassian, V., Lerat, J., and Michel, C.: Has land cover a significant impact on mean annual streamflow? An international assessment using 1508 catchments, J. Hydrol., 357, 303–316, 2008.

Peel, M. C., Chiew, F. H. S., Western, A. W., and McMahon, T. A.: Extension of Unimpaired Monthly Streamflow Data and Regionalisation of Parameter Values to Estimate Streamflow in Ungauged Catchments. Report prepared for the Australian National Land and Water Resources Audit., Centre for Environmental Applied Hydrology, The University of Melbourne, 2000.

Santhi, C., Allen, P. M., Muttiah, R. S., Arnold, J. G., and Tuppad, P.: Regional estimation of base flow for the conterminous United States by hydrologic landscape regions, J. Hydrol., 351, 139–153, 2008.

Schoups, G., van de Giesen, N. C., and Savenije, H. H. G.: Model complexity control for hydrologic prediction, Water Resour. Res., 44, W00B03, doi:10.1029/2008WR006836, 2008.

Sivapalan, M., Takeuchi, K., Franks, S. W., Gupta, V. K., Karambiri, H., Lakshmi, V., Liang, X., McDonnell, J. J., Mendiondo, E. M., O'Connell, P. E., Oki, T., Pomeroy, J. W., Schertzer, D., Uhlenbrook, S., and Zehe, E.: IAHS Decade on Predictions in Ungauged Basins (PUB), 2003–2012: Shaping an exciting future for the hydrological sciences, Hydrol. Sci. J., 48, 857–880, doi:10.1623/hysj.48.6.857.51421, 2003.

Tallaksen, L. M.: A review of baseflow recession analysis, J. Hydrol., 165, 349–370, 1995.

van Dijk, A. I. J. M., Hairsine, P. B., Arancibia, J. P., and Dowling, T. I.: Reforestation, water availability and stream salinity: A multi-scale analysis in the Murray-Darling Basin, Australia, Forest Ecol. Manag., 251, 94–109, 2007.

Wagener, T. and Wheater, H. S.: Parameter estimation and regionalization for continuous rainfall-runoff models including uncertainty, J. Hydrol., 320, 132–154, 2006.

Weisman, R. N.: The effect of evapotranspiration on streamflow recession, Hydrol. Sci. Bull., XXII, 371–377, 1977.

Wittenberg, H.: Baseflow recession and recharge as nonlinear storage processes, Hydrol. Process., 13, 715–726, 1999.

Wittenberg, H. and Sivapalan, M.: Watershed groundwater balance estimation using streamflow recession analysis and baseflow separation, J. Hydrol., 219, 20–33, 1999.

Zecharias, Y. B. and Brutsaert, W.: Recession characteristics of groundwater outflow and baseflow from mountainous watersheds, Water Resour. Res., 24, 1651–1658, 1988.

Zhang, L., Hickel, K., Dawes, W. R., Chiew, F. H. S., Western, A. W., and Briggs, P. R.: A rational function approach for estimating mean annual evapotranspiration Water Resour. Res., 40, W02502, doi:10.1029/2003WR002710, 2004.